Department of Pesticide Regulation

Mary-Ann Warmerdam
Director

Edmund G. Brown Jr.
Governor

M E M O R A N D U M

TO: Randy Segawa
Environmental Program Manager I
Environmental Monitoring Branch

FROM: Frank Spurlock, Ph.D. *Original signed by*
Research Scientist III
Environmental Monitoring Branch
916-324-4124

DATE: January 31, 2011

SUBJECT: SIMULATION OF THREE UNTARPED1,3-DICHLOROPROPENE FLUX STUDIES USING HYDRUS

ABSTRACT

Post-application 1,3-dichloropropene (1,3-D) volatilization data from three untarped field studies were simulated using HYDRUS vadose zone models. The volatilization fluxes in the original studies were estimated using the aerodynamic (AD) method. HYDRUS simulated fluxes were calculated using measured or independently estimated input data with the exception that the soil bulk degradation coefficient was an adjustable parameter. The best-fit soil degradation half-lives were similar across all three studies, ranging from 5.1 d to 5.8 d, even though soil types were quite different. The timing and magnitude of HYDRUS-simulated 1,3-D flux densities were within the range of uncertainty of the AD-estimated flux densities in one of the three studies. The peak AD-estimated flux density in the second study occurred several days before the peak HYDRUS modeled flux density, and the cumulative modeled flux was similarly delayed. In contrast, the peak AD-estimated flux and cumulative fluxes in the third study were much later than their corresponding HYDRUS-estimates. Several potential reasons for the deviations between AD-estimated and HYDRUS-modeled flux were identified, including:

- Uncertainty in the AD-estimated fluxes.
- Uncertainty in soil effective vapor phase diffusion coefficients. These coefficients are calculated internally by the HYDRUS based on a user-specified tortuosity model. Those tortuosity models are subject to prediction error, particularly in the wet soil range.
- Inadequate characterization of soil physical properties due to inadequate pre-application soil sampling, leading to inaccurate model parameterization or initial conditions.
- Extensive spatial variability in soil properties.
- Sampling error in field measured concentrations (contributing to flux estimation error).

In future studies, some of these problems can be minimized by increased sampling to better characterize soil properties and water content. However, other problems, such as those related to extreme spatial variability, may require alternate modeling approaches such as probabilistic

modeling. Across all three studies, peak modeled fluxes were 71% of the AD-estimated fluxes (range 53 – 81%). However, the AD-estimates themselves are subject to substantial error. Additional work to understand the magnitude and sources of flux estimation error would be useful.

INTRODUCTION

DPR has been evaluating the one- and two-dimensional HYDRUS vadose transport models (Šimunek et al., 2005, 2006) for simulating fumigant volatilization from soil. The Department of Pesticide Regulation recently engaged the services of Dr. Jirka Šimůnek (model author) to implement modifications enhancing the ability of HYDRUS to simulate fumigant fate and transport. The computational testing of the modified programs has been satisfactorily completed (Spurlock et al., 2010). This study is the first in a series of subsequent evaluations of HYDRUS ability to simulate field data. The objectives of this study were to (a) gain experience in simulating actual field data sets, (b) evaluate HYDRUS input data requirements relative to data reported in relatively complete and well-documented fumigant flux studies, (c) test the ability of the HYDRUS models to simulate vadose transport processes, and (d) investigate potential problems in evaluating model goodness of fit.

Three 1,3-D untarped fumigant applications were simulated using HYDRUS (Table 1). The studies were all conducted in California by Dow Elanco (currently known as Dow Agrosciences) in the early 1990's (Knuteson et al., 1992a, 1992b; Knuteson et al., 1995). These studies were chosen because they were relatively complete studies that included chemistry QA/QC data, initial and end-of-study soil-water content measurements, and a modicum of site-specific soil characterization data. The studies were conducted near Salinas (study #1), Madera (study #2) and Imperial County (study #3), and represented a range of soils: sandy loam, loam and clay loam, respectively. In all studies, the 1,3-D flux was estimated from on-sight measured air concentrations and meteorological data using the AD flux estimation method.

Table 1. Summary of 1,3-D untarped fumigation studies

Study	Soil Type	Application Type	Model	Duration
#1 - Salinas (Knuteson et al., 1992a)	Sandy Loam	Broadcast shank, 16 – 20 in depth, 10 acres	HYDRUS-1D	14 days
#2 - Madera (Knuteson et al., 1995)	Loam	Bedded row shank application, 20-22 in depth, 10 acres	HYDRUS2/3 D	21 days
#3 - Imperial (Knuteson et al., 1992b)	Clay Loam	Broadcast shank, 16 – 20 in depth, 15 acres	HYDRUS-1D	8 days

II. RESULTS

A. Salinas study

1. Soil water pressure head and water contents

Two sets of measured data were available for evaluating HYDRUS simulation of soil-water dynamics: (a) daily tensiometer measurements of soil-water pressure head at 15 cm and 30 cm depths and (b) end of experiment (14d) average soil water content at 015 cm, 15 – 30 cm and 30 – 45 cm depths.

There was a small systematic deviation between modeled and measured soil water pressure heads at the 15 cm depth (Figure 1a). The model initial conditions were defined as the soil water content measured on day zero (Appendix 1). These were translated into pressure head internally by the model using the soil-water retentivity function. Observation nodes were defined in the model to obtain modeled pressure heads on each day at the 15cm and 30 cm depths. The measured 15 cm tensiometer data were reported up to day 9, after which the tensiometer failed. At the 30 cm depth, modeled pressure heads were similarly more negative than measured. However, in both cases the deviations were relatively minor. The mean 14 day 30 cm water contents calculated from measured and modeled pressure head data (Figure 1b) using the 15.2 – 30.4 cm van Genuchten (van Genuchten, 1980) parameters were 0.158 and 0.140, respectively (Appendix 1, Table A-4). As point of reference, this difference in mean water content corresponds to an estimated 13% larger effective gas phase diffusion coefficient for the modeled pressure head relative to the measured pressure head. This difference is due to tortuosity effects, and was calculated using the Water-induced Linear Release (WLR) tortuosity model (Moldrup et al., 2000).

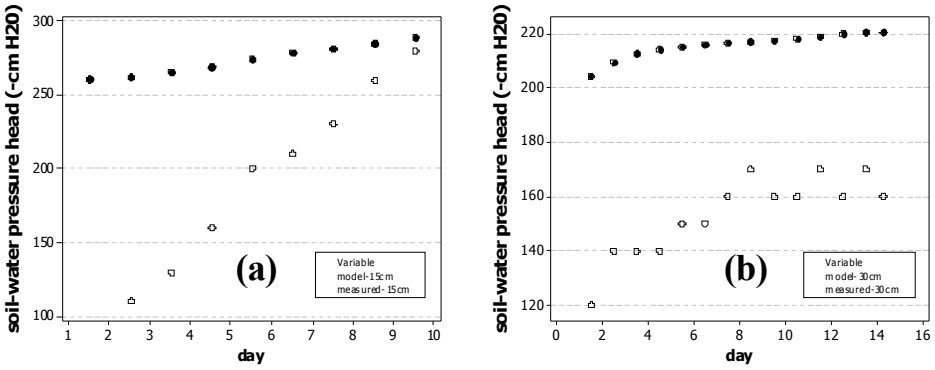

Figure 1. **(a)** measured and simulated soil-water pressure heads at 15 cm depth. Tensiometer malfunctioned during experiment so data were only reported for days 2 – 9 and **(b)** measured and simulated soil-water pressure heads at 30 cm depth.

The modeled end of simulation 0 – 15 cm, 15 – 30 cm, and 30-45 cm water contents all fell within the range of measured values from the 4 cores taken at the end of the experiment (Figure 2). In light of the limited measured soil data for estimating retention curve parameters, the differences between measured and simulated soil-water pressure heads in Figure 1 are relatively small. In addition, the agreement between simulated and measured 14 day end-of-study soil water contents are quite good.

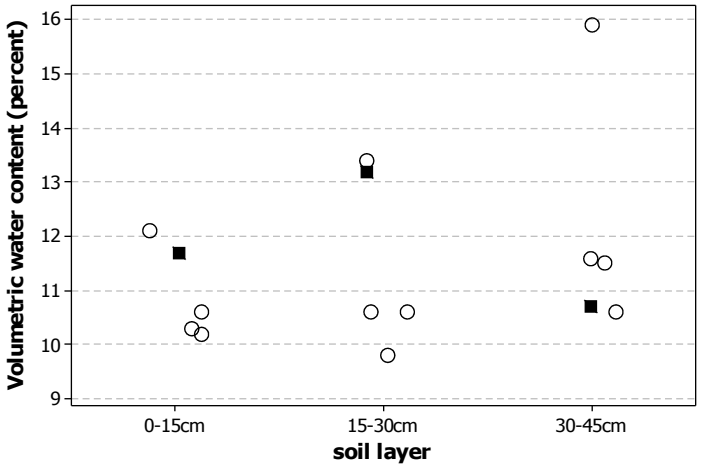

Figure 2. Measured and simulated soil water contents at end of experiment (14 days). Measured values for each core are open circles, simulated water contents are average for 52 nodes within the respective depth layer, shown by filled squares.

2. Optimization for bulk soil degradation coefficient

The best-fit 1,3-D degradation rate constant of 0.12 day^{-1} ,(0.117, 0.122, 95% CI) was determined by minimizing the squared residuals between AD-estimated and modeled cumulative flux. This rate constant corresponds to a fitted half-life of 5.8 days, comparable to reported 1,3-D half-lives estimated in other studies (e.g. van Dijk, 1980; 4.2 - 18.7 days; Zheng et al., 2003; 5.2 – 6.4 days; Kim et al., 2003; 6.5 – 7.4 days). The cumulative flux modeled using this rate constant agreed well with AD-estimated cumulative flux profile throughout the study (Figure 3). AD-estimated flux densities for the first sampling period are not comparable to modeled values because the fumigant application was in progress during the first half of that first 6 hr sampling interval. Over the remaining 41 sampling periods, the absolute percent deviation between modeled and AD-estimated period average flux densities F_i ranged from 1 to 197 percent (period 4), with a mean of 31.3% (Figure 4). The deviations at each sampling period i were calculated as:

$$[1] \qquad \varepsilon_i = \left| \frac{F_{i,modeled} - F_{i,estimate}}{F_{i,estimate}} \right| \times 100$$

where $F_{i,estimate}$ and $F_{i,model}$ are the AD-estimated and modeled flux densities and ε_i is the deviation, or percent error, between modeled and estimated flux densities.

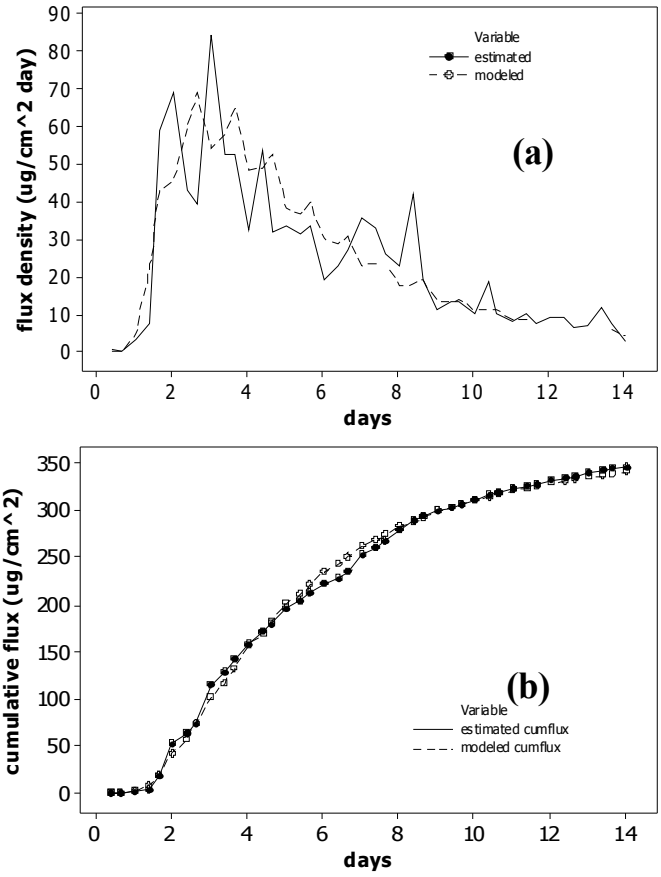

Figure 3. Salinas data: HYDRUS simulated and AD-estimated **(a)** flux densities and **(b)** cumulative flux. Application occurred between 0.3 and 0.5 days.

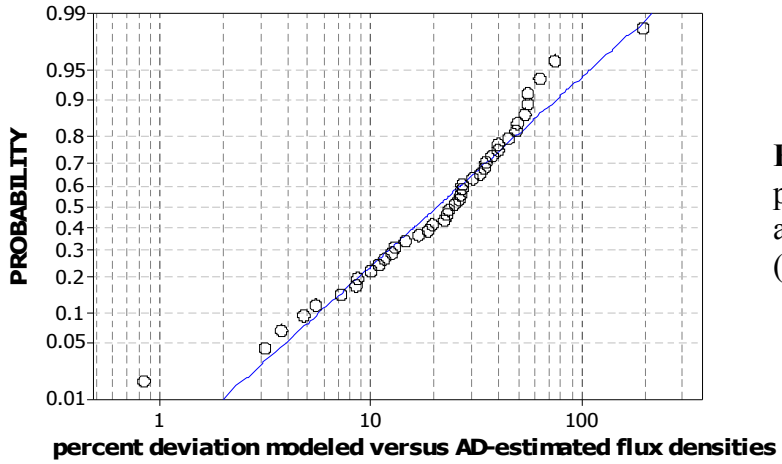

Figure 4. Cumulative frequency of percent deviations between modeled and AD-estimated flux densities (Eq. 1).

3. Assessing goodness-of-fit

The percent deviation statistics reflect the difference between modeled and AD-estimated flux densities, but do not measure how well the model predicts actual flux. This is because the AD method itself is an estimate of flux which is subject to error. The relationship between AD-estimated, modeled and "true" or actual flux densities at any sampling interval *i* is

[2]
$$F_{i,actual} = F_{i,estimate} + \varepsilon_{i,estimated}$$
$$= F_{i,model} + \varepsilon_{i,model}$$

where $F_{i,actual}$, $F_{i,estimate}$ and $F_{i,model}$ are the actual, AD-estimated and modeled flux densities, respectively, and $\varepsilon_{i,estimate}$ and $\varepsilon_{i,model}$ are the estimate and model errors. The $\varepsilon_{i,model}$ contains potential contributions from model inadequacy (inaccurate or incomplete specification of various and fate processes) or inaccurate parameterization. The $\varepsilon_{i,estimate}$ potentially includes analytical chemistry error, failure of the physical system to meet assumptions of the underlying flux estimation model, or inadequacy of the flux model.

The most direct approach for evaluating a model's performance relative to the real world is to compare $F_{i,model}$ and $F_{i,actual}$ to obtain estimates of $\varepsilon_{i,model}$, and evaluate the magnitude of that error relative to $F_{i,actual}$ (Eq. 2). However, in this case $F_{i,actual}$ is unknown.

The choice of sign for the error terms in Eq. 2 is arbitrary, so the relationship between estimated and modeled flux may be written

[3]
$$F_{i,estimate} = F_{i,model} + \varepsilon_{i,model} + \varepsilon_{i,estimate}$$
$$= F_{i,model} + \varepsilon_{i,total}$$

where $\varepsilon_{i,total}$ is the "total" error, containing contributions from both $\varepsilon_{i,estimate}$ and $\varepsilon_{i,model}$. If $\varepsilon_{i,estimate} << \varepsilon_{i,model}$ generally, then $\varepsilon_{i,model} \approx \varepsilon_{i,total}$ and we can assess model goodness of fit using the $F_{i,estimate}$ as a surrogate for $F_{i,actual}$. On the other hand, if the magnitudes of $\varepsilon_{i,estimate}$ and $\varepsilon_{i,model}$ are comparable, differences between modeled and estimated fluxes will include both modeling and estimate error. In that case meaningful assessment of a model performance relative to reality requires knowledge of $\varepsilon_{i,estimate}$ (Eq. 3).

Majewski (1997) described a method for estimating uncertainty in AD flux estimates. The AD model relies on assumptions that both windspeed and concentration vary linearly with the logarithm of height above the ground surface. The AD method also assumes certain functional relationships between windspeed, temperature and the atmospheric thermal stability terms. Majewski (1997) estimated the error in calculated windspeed and concentrations based on regression error (windspeed on log[height], concentration on log[height]) for those respective data

at each sampling interval. The windspeed regression error was also allowed to propagate through the thermal stability relationships used to ultimately estimate flux. The analysis assumed that the windspeed and concentration errors were independent, and Normal-based error propagation methods were used to calculate the overall coefficient of variation (CV = σ/μ * 100) of $F_{i,estimate}$ at each of 31 sampling intervals. Other sources of error, such as those related to duration of sampling periods, spatial variability or other deviations from AD method assumptions were not considered in Majewski's analysis.

After removal of the first sampling interval where the fumigant application was still underway, and an apparent outlier of 181% on one of the day 6 intervals, the estimated coefficients of variation across the 29 remaining sampling intervals ranged from 10% to 81%, with a mean of 37% (Figure 5).

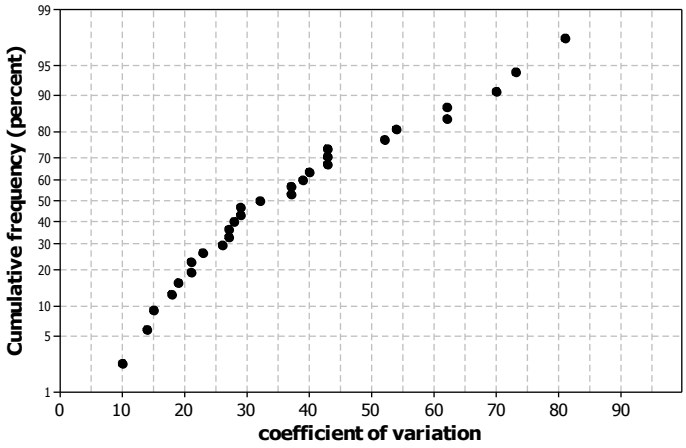

Figure 5. Estimated coefficients of variation (= σ/μ * 100) of flux density estimated by Majewski (1997) for 29 sample intervals. The fumigant was methyl bromide and the aerodynamic method was used to estimate flux.

There were no detailed windspeed or temperature vs. height data reported by Knuteson et al. (1992a) so Majewski's error estimation method could not be directly applied. Are Majewski's error estimates applicable to the Salinas study? The similarities between the Salinas and Majewski (1997) AD flux studies were that:

- Both occurred during fall months in the Salinas Valley.
- Daily maximum and minimum temperatures were comparable, with median daily high and low air temperatures of 76F versus 70F and 52F versus 48F for the Knuteson et al. (1992a) and Majewski (1997) studies, respectively.
- Median daily mean windspeeds were similar at 7 mph versus 5.5 mph in the Knuteson et al. (1992a) and Majewski (1997) studies, respectively.

Important differences between the studies were

- Majewski (1997) monitored a methyl bromide application instead of 1,3-D as in the - Salinas study. -
- The soil types were different. Majewski's study took place in a silty clay loam, whereas the Knuteson et al. (1992a) study soil was in a fine sandy loam.

Two of three error propagation terms in Majewski's analysis (1997) are related only to error in the windspeed vs height regression. Fumigant type would have no effect on this source of error, although fumigant type might have an effect on chemical analytical variability. The potential effect of soil type on errors, if any, is unknown. At minimum it is evident that $\varepsilon_{i,measured}$ can be a substantial contributor to $\varepsilon_{i,total}$. Assuming Majewski's error estimates are representative, the deviations between HYDRUS modeled and AD-estimated flux densities observed here (mean = 31%; Figure 4) are within the range of uncertainty in the AD-estimated fluxes (i.e., mean = 37% in Majewski's analysis); the model could not have performed better relative to the "field data" in this case.

B. **Madera study**

In the Madera study (Knuteson et al., 1995), 1,3-D was applied via subsurface shank injection at the ~20 – 22 in (51 – 56 cm) depth. The rows were formed into beds during the fumigant treatment by a tractor following the fumigation rig that also pulled a solid roller to compress and finish the bed tops. The modeling domain was two-dimensional (Figure A-2, Appendix 1) and HYDRUS 2/3D was used for modeling flux.

1. Soil water content

No field measured pressure head data were collected. However, daily cores were taken and analyzed for water content over the course of the study. In the first and third layers (0 – 15 cm and 30 – 45 cm, respectively), modeled and measured volumetric water content θ agreed well over duration of the study (Figure 6a). However, in layers 2 and 4 (15 – 30 cm and 45 – 60 cm, respectively), the modeled θ were consistently lower than measured, with $\Delta\theta$ = (measured – modeled) increasing from 0 or slightly negative to nearly 0.05 by the end of the study (Figure 6b). The primary effect of low simulated θ on fumigant transport is to enhance the modeled rate of fumigant transport. This occurs due to the nature of the relationships between water content, tortuosity and fumigant effective diffusion coefficient (Spurlock, 2008). Thus, based on the simulated water content data, the expectation is that modeled volatilization might be faster than actual volatilization.

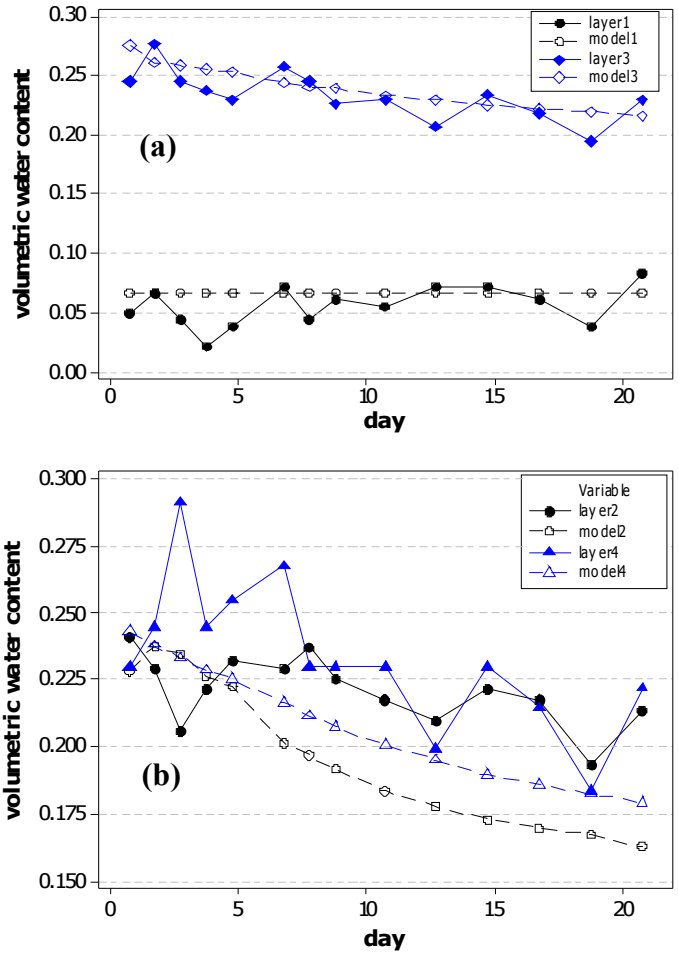

Figure 6. Measured (denoted layer 1 – layer 4) and modeled (denoted model 1 – model 4) volumetric soil-water content (cm^3 H_2O cm^{-3} bulk soil) throughout the study. (a) measured and modeled data for layer 1 (0 – 15.2 cm) and layer 3 (30.4 – 45.6 cm), and (b) measured and modeled data for layer 2 (15.2 – 30.4 cm) and layer 4 (45.6 – 60.8 cm). The stated fumigant application depth was 46 – 56 cm.

2. Fitting of bulk soil degradation coefficient

As with the fitting of the Salinas data, all input variables except the soil bulk degradation coefficient were fixed. The WLR tortuosity model was assumed. Selection of the "best-fit" degradation coefficient was achieved by trial and error with only a few iterations. The criteria for best-fit was the minimum difference between measured and observed 21 day 1,3-D cumulative flux. The result was a best-fit degradation coefficient corresponding to a 5.6 day 1,3-D soil half-life, comparable to reported 1,3-D half-lives observed or estimated in other studies (e.g. van Dijk, 1980; 4.2 – 18.7 days; Zheng et al., 2003; 5.2 – 6.4 days; Kim et al., 2003; 6.5 – 7.4 days).

While the AD-estimated and HYDRUS fitted cumulative fluxes were essentially identical at 21 days (Figure 7b), deviations between AD-estimated and modeled flux density time series were striking (Figure 7a); 1,3-D volatilization as estimated from the AD model was much more rapid

than that predicted by HYDRUS (Figure 7). The deviations were systematic, where AD-estimated flux densities were much greater than modeled prior to day 5, and vice-versa after day 5. Consequently the deviations are not attributable to random AD-flux estimation error. 1,3-D volatilization was also much more rapid in the Madera study than in Salinas (Figure 8).

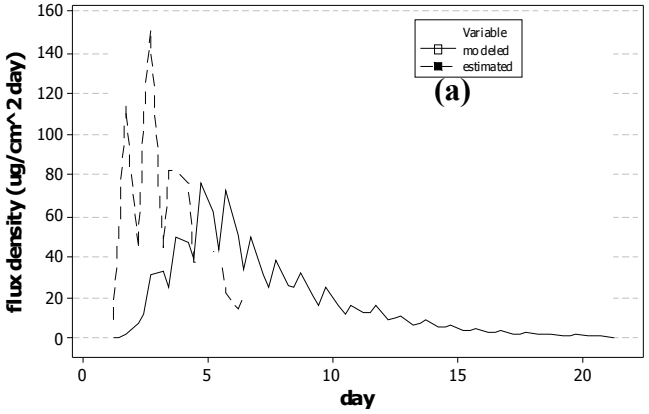

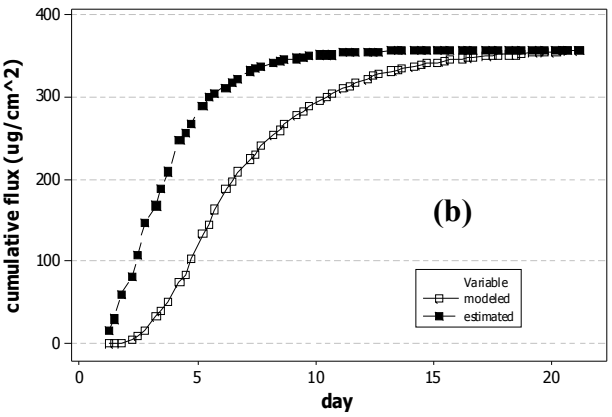

Figure 7. AD-Estimated and modeled 1,3-D **(a)** flux densities and **(b)** cumulative - flux for the Madera data. The application began at approximately 1500 hours (0.63 day) and was completed at 1900 hours (0.79 day).

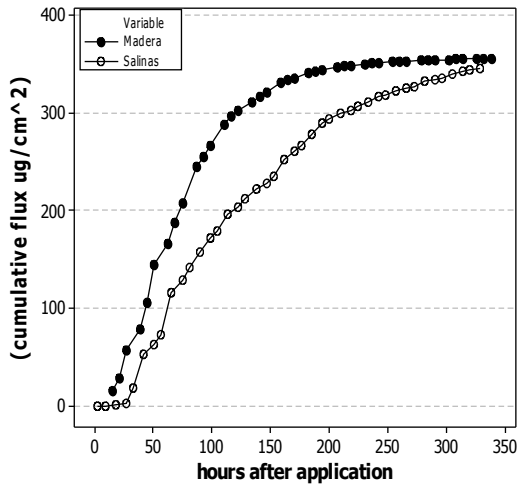

Figure 8. Comparison of AD-estimated cumulative flux profiles in Madera and Salinas studies. Application rates were essentially equal; 116 lbs/acre in Madera as compared to 121 lbs/acre in Salinas.

3. Comparison of Salinas and Madera Studies

In an attempt to understand the difference in 1,3-D volatilization between the Madera and Salinas studies, the experiemnetal conditions were compared. The principal differences between were:

Soil type – The Salinas soil was a sandy loam, coarser than the Madera loam soil. Other factors being equal, gas phase transport is generally more rapid in coarse soils due to their larger pore sizes. Thus, this would generally favor faster volatilization in Salinas, all other factors being equal.

Soil-water content – The initial 0-15 cm volumetric soil water content θ was much lower in Madera (0.05 – 0.06) as compared to Salinas (0.15). In contrast, the 15 – 30 cm layer had an initial θ of 0.24 and 0.12 for the Madera and Salinas studies, respectively. In both cases the 0 – 15 cm and 15 – 30 cm layers were above the fumigant injection depth. Consequently the effect of water content on initial overall rate of fumigant diffusion in the two top layers is mixed; the dry Madera top layer would favor more rapid gas-phase movement than in the Salinas soil, whereas the wetter Madera second layer would have the opposite effect. Thus, the effect of soil water content is equivocal.

Depth and geometry of application – Depth of injection was 45 cm below ground level in the Salinas study (Figure A-1, Appendix 1), whereas the Madera application was 53 cm below the top of the bed (Figure A-2, Appendix 1). However, because of the application geometry, the minimum distance from center of shank injection to the soil surface was 38 cm in the Madera study (center of injection to closest furrow edge) as compared to 45 cm for the Salinas application. All other factors being equal, this 15% shorter macroscopic diffusion path length would favor slightly faster volatilization in the Madera study as compared to Salinas.

Weather – Conditions were somewhat drier and warmer in Madera as compared to Salinas, but the differences were not great (Table 2). Mean daily windspeeds were comparable at 6 versus 7 mph at Madera and Salinas, respectively.

Barometric pressure – Barometric pressure fluctuations were much greater in the Madera study as compared to Salinas. This was particularly true for the first 24 – 48 hours post-application (Figure 9) when rapid volatilization was observed in Madera. A transport mechanism that is known to be important in fractured porous media - such as rock - is advective transport due to barometric pressure fluctuations. This mechanism is sometimes called “barometric pumping.” However, there is far less agreement on the importance of barometric pumping as a transport mechanism in more homogeneous media such as sandy soils. While Chen et al. (1995) hypothesized that advective transport was often responsible for poor

performance of diffusion-based models in simulating fumigant transport, others have concluded that the contribution of barometric pumping to volatile pollutant transport in soils is "often negligible" as compared to diffusion (Atteia and Hohener, 2010).

Although barometric pressure variation during the first few days of the Madera study were much greater than during the Salinas study, it is doubtful that barometric pumping was responsible for rapid 1,3-D volatilization in Madera for two reasons. First, the overall magnitude of pressure changes during days 1 and 2 were relatively low, at 2.4 and 3.4 mbar, respectively. These are typical deviations for daily diurnal summer pressure changes in California's Central Valley, and much smaller in magnitude than changes that have been implicated in volatile chemical vadose transport in soils (Auer et al., 1996; Massman and Farrier, 1992). Most important is that the net Madera pressure changes on day 1 and 2 were positive. The effect of such changes would have been to decrease emissions on these two days in the Madera study (Auer et al., 1996), the opposite of what was observed.

Table 2. Selected weather variables for days 1-5 of the Salinas and Madera 1,3-D flux studies. Data from weather stations Madera.T, Fresno.A and Salinas.A.

Day no.	max. temp. (F)	min. temp. (F)	wind speed (mph)[A]	max. relative humidity[A]	min. relative humidity[A]
Salinas					
1	75	52	7	88.6	55.7
2	70	52	6	86.2	54.7
3	77	52			
4	80	50	6	79.6	31.4
5	83	51	8	80.4	25.4
Madera					
1	80	46	4	85.7	34
2	78	60	7	73	27.5
3	80	48	9	81.4	20.5
4	77	51	7	87.2	23.5
5	89	49	3	85	24.2

[A] Madera wind speed and humidity data from weather station Fresno.A

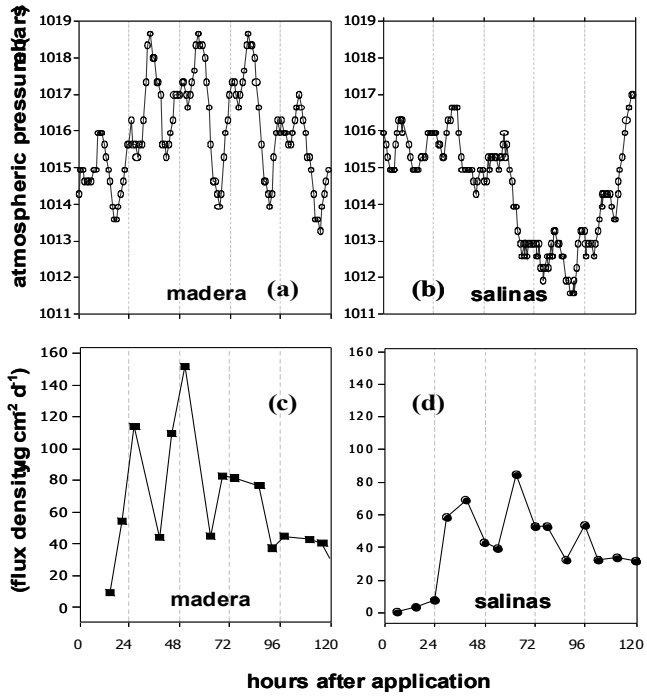

Figure 9. Barometric pressure in (a) Madera and (b) Salinas studies, and AD-estimated flux densities in (c) Madera and (d) Salinas stuidies during the first 120 hours of each study. Salinas data from Salinas Municipal Airport (KSNS), Madera data from Fresno Yosemite International Airport (KFAT). Barometric pressure data adjusted to sea level, downloaded from *wunderground.com*.

4. Comparison of AD-estimated and HYDRUS-modeled Madera fluxes

Sustained rapid 1,3-D volatilization from soil relative to model results could only occur in conjunction with rapid 1,3-D diffusive movement in the soil. The magnitude of that "enhanced" mobility is illustrated by answering the question "*theoretically, what gas phase diffusion coefficient is required for the modeled cumulative flux data to match the AD-estimated data*?" Figure 10 compares AD-estimated and HYDRUS-modeled flux for the identical Madera scenario conditions and solute properties as in Figure 7, except that the 1,3-D diffusion coefficient in air D_0 used for modeling was 18,000 cm^2 day^{-1} instead of the true D_0 of 6886 cm^2 day^{-1}. This implies that the actual effective rate of diffusion in the field was ~ 2.6 (=18,000/6886) times greater than that predicted by HYDRUS.

Although the solute gas phase diffusion coefficient D_0 is specified as input to HYDRUS, program calculations actually use the solute -bulk soil diffusion coefficient D_s to calculate volatile solute diffusive movement. Thorbjørn et al. (2008) summarize a variety of empirical models for describing gaseous diffusion coefficients in soil. These include the Water-induced WLR model implemented in HYDRUS and used here.

[4] - $$\frac{D_s}{D_o} = \frac{a_v^{2.5}}{\theta_s}$$

where θ_s is saturated water content (assumed to represent total porosity), and a_v is the volumetric air-filled porosity, typically taken as (θ_s - θ). The soil diffusion coefficient D_s is always less than D_o because of the reduction in available cross-sectional area available for diffusion in a porous media, and disconnectivity and tortuosity of the air-filled pores. D_s is essentially a volume average diffusion coefficient in the sense that it represents the equivalent overall diffusion coefficient for the solute as if diffusive transport were occurring *throughout the entire cross-section of the medium* instead of just in the air-filled pores.

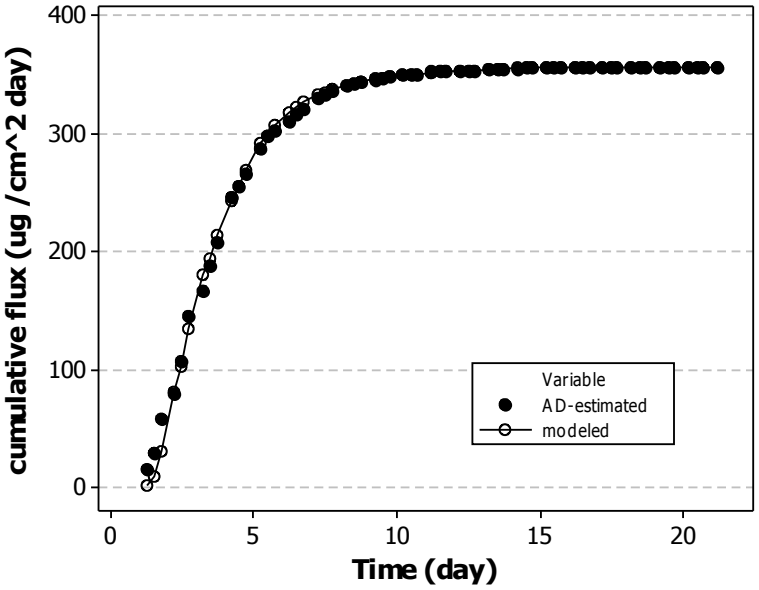

Figure 10. AD-estimated Madera cumulative flux and HYDRUS-modeled cumulative flux for an imaginary solute with gas phase diffusion coefficient $D_0 = 2.61 * D_{0,\ 1,3\text{-}D} = 2.61 * 6886 = 18{,}000$ $cm^2\ day^{-1}$.

Figure 11 is a modification of Figure 7b in Thorbjørn et al.'s (2008) recent comparison of soil diffusion models. They compared the ability of several tortuosity models to predict D_s using 810 diffusion measurements obtained from a variety of undisturbed and repacked soil samples. The blue lines superimposed on the figure show the predicted ratio D_s/D_o for the upper 4 Madera soil layers based on average water content throughout the study (Figure 6) and θ_s (Table A-6, Appendix 1). The relatively dry upper 0 15 cm layer yields a predicted D_s/D_o of 0.33, while the lower layers fall in the range of 0.03 – 0.04. Based on Thorbjørn et al.'s (2008) data, it is doubtful that the actual 0 – 15 cm D_s/D_o could be 2.6 times greater than the WLR D_s/D_o prediction of 0.33. However, in the deeper soil layers where $0.03 \leq D_s/D_o \leq 0.04$, it appears that measured D_s/D_o could easily be a factor of 2.6 greater than the predicted value based on the observed variability. Thus, variability in soil diffusion coefficient could be a primary contributor to rapid 1,3-D volatilization

relative to the Salinas study, and the corresponding prediction error would also explain the rapid volatilization as compared to HYDRUS.

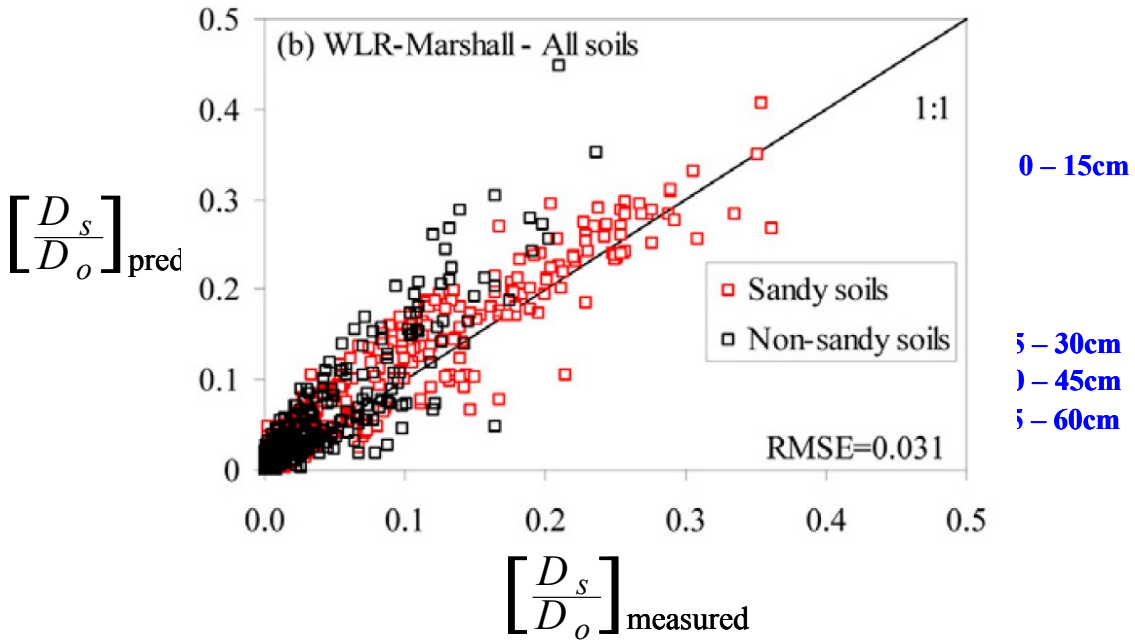

Figure 11. Predicted versus measured D_s/D_0 ratios, where D_s is the effective gas phase diffusion coefficient in soil and D_o is the gas phase diffusion coefficient in free air. Predictions are based on the WLR model (N=810). Taken from Figure 7b of Thorbjørn et al. (2008). The plot illustrates potential for high relative prediction errors, particularly for low D_s/D_o ratios (i.e. at high water contents).

5. Potential role of modeling domain mis-specification

Cryer and Wesenbeeck (2009), and more recently Wang et al. (2010), hypothesized that in some cases, a region known as the "shank trace" is created during shank application of fumigants. This region is characterized by low soil bulk density, high porosity and enhanced fumigant diffusive transport. While intuitively appealing, there are essentially no peer-review data that document the presence of shank traces or their characteristics (Johnson, 2008). Without such data, it is impossible to determine if, or under what conditions (e.g. soil texture, water content) shank traces might be formed, or what size or hydraulic characteristics such a shank trace might possess.

In the illustrative example shown in Figure 12, a 10 cm wide "shank trace" extending from the soil surface down to the fumigant injection point is arbitrarily assumed to possess the same properties as the blue (highly permeable) surface bed layer of soil (Appendix, Table A-5). A simulation using the shank trace scenario and the 5.6 day bulk soil half-life previously estimated fits the

AD-estimated Madera flux data quite well (Figure 13). However, with no actual field measurements or observations that support the presence of a "shank trace" in the Madera study, the idea remains a hypothesis to be investigated further.

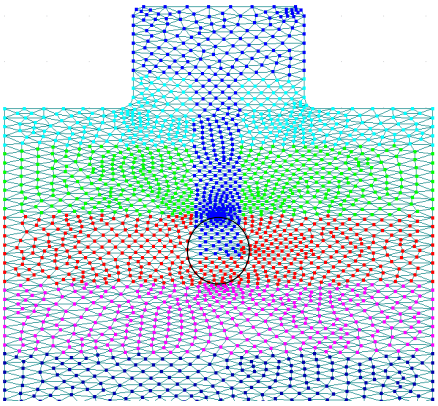

Figure 12. Illustrative example of a "shank trace" scenario. Different colors are soil regions with different characteristics such as hydraulic characteristics, tortuosity, and gas permeability.

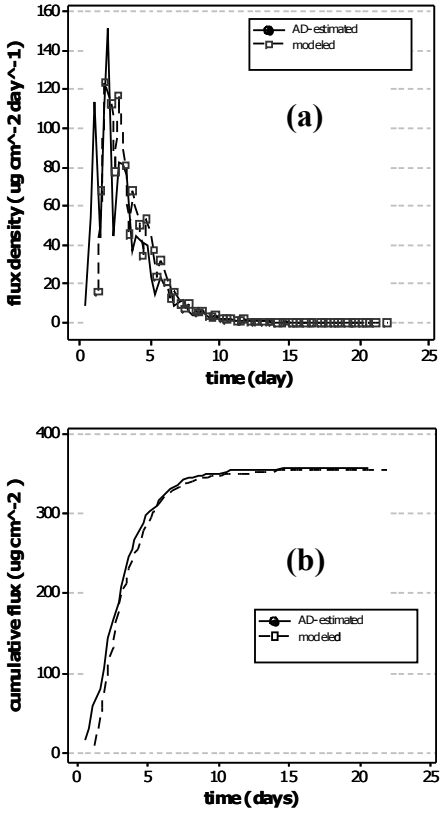

Figure 13. AD-estimated and HYDRUS modeled **(a)** flux density and **(b)** cumulative flux data. HYDRUS simulation *assumes* the presence of a "shank trace" (see text).

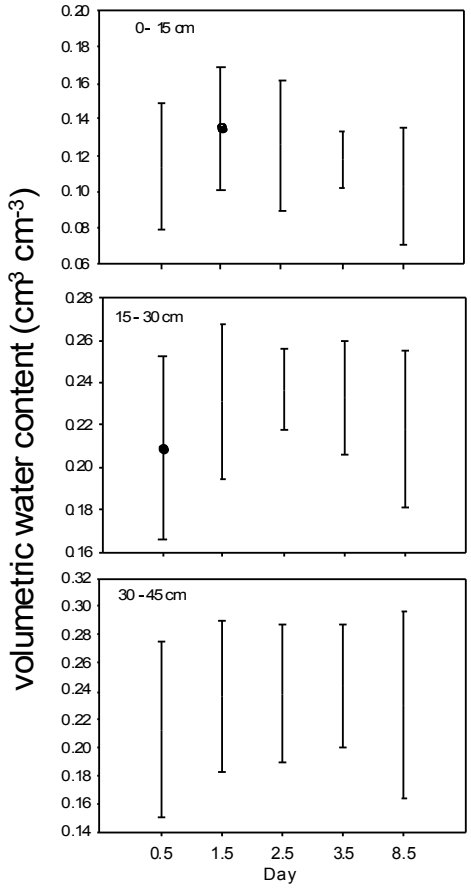

C. Imperial study

Soil samples were taken for water content for the first 4 days and at the end of the Imperial study. Eight cores (45 cm x 3 segments) were taken at each sampling time. HYDRUS over-predicted the 0 – 15 cm water content during the last half of the study, while the two deeper layers showed the opposite effect (Figure 14). Noteworthy was the spatial variability in volumetric soil-water contents. Coefficients of variation in measured water contents ranged from 8% – 31%, with means of 26%, 15% and 21% for the 0 – 15 cm,
15 – 30 cm and 30 – 45 cm layers, respectively. This wide range illustrates substantial variability across the plot, indicating that a single set of hydraulic parameters is inadequate to simulate soil-water dynamics in this study. Diffusive transport is sensitive to soil water content. A single deterministic simulation will likely be unable to accurately describe fumigant volatilization at this site. It is also important to note that the volumetric water content data were calculated from measured gravimetric water content data and bulk densities. Because the the bulk density data were collected at different times and locations than the gravimetric water samples, sampling error also contributes to total volumetric water content error.

Figure 14. Simulated (open triangles) and measured (solid symbols with error bars, N=8) volumetric water contents in the Imperial study.

Based on the AD-estimated flux density, 1,3-D volatilization was very slow in the Imperial study. The peak estimated flux density occurred almost seven days after application (Figure 15a). This result was unusual, as peak flux in nearly all untarped or tarped 1,3-D studies occur in the first day or two after application (Wang et al., 2000; Thomas et al., 2003; Wesenbeeck et al., 2007; Cryer and Wesenbeeck, 2009).

Local barometric pressure was gradually decreasing on days 1 – 5 of the study which, in theory, should promote more rapid 1,3-D volatilization (Figure 15b). Beginning on day 5, 1,3-D flux density increased, reaching a peak on day 7. At the same time barometric pressure was increasing

which should have decreased volatilization if anything. Thus, barometric pressure effects were not responsible for the apparent slow 1,3-D volatilization in the Imperial study.

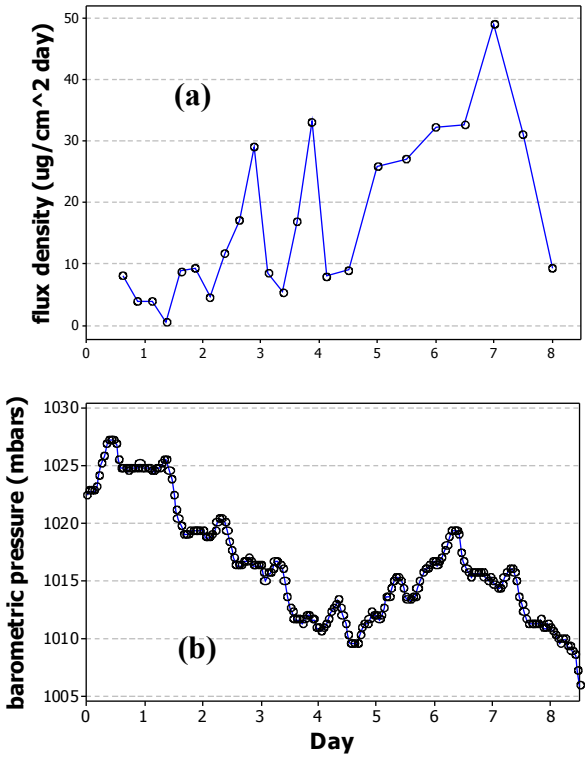

Figure 15. **(a)** AD-estimated flux density, and (b) hourly barometric pressure (Imperial Airport, KIPL) during Imperial 1,3-D fumigation study. Barometric pressure data adjusted to sea level, downloaded from <*wunderground.com*>..

The best-fit 1,3-D soil degradation coefficient was chosen by minimizing the difference between end-of-study AD-estimated and modeled cumulative flux (Figure 16b). The corresponding best-fit 1,3-D soil-half life was 5.1 days, quite similar to half-lives estimate in the Salinas and Madera studies (5.8 and 5.6 days, respectively). However, overall agreement between AD-estimated and HYDRUS-estimated flux densities was poor (Figure 16a). The deviations between the modeled and the AD-estimated flux densities were systematic; nearly all modeled fluxes prior to day 4.5 were greater than AD-estimated, with the opposite being true after day 4.5. Consequently the deviations between modeled and estimated are not attributable to random AD-flux estimation error as appeared to be the case in the Salinas study.

One interesting component of the Imperial field study was the inclusion of (a) replicate air samplers at the 33 cm and 90 cm heights on the primary air sampling mast used to measure air

concentrations used in the AD-estimation method, and (b) two replicate air sampling masts also with air samplers at the 33 cm and 90 cm heights. The coefficients of variation (CV) between replicates within mast samplers ranged from 3 percent to 93 percent, with a mean of 21 percent. Mean CVs for the between-mast sample replicate concentrations over the same sampling period were 21 percent and 25 percent at the 33 cm and 90 cm height, respectively. These data indicate substantial $\varepsilon_{i,estimate}$. However, deviations between modeled and AD-estimated values were clearly systematic. Thus, while there was no doubt that sampling error contributed to error in the AD-flux density estimates, systematic deviations between modeled and AD-estimated flux densities indicate other sources of error.

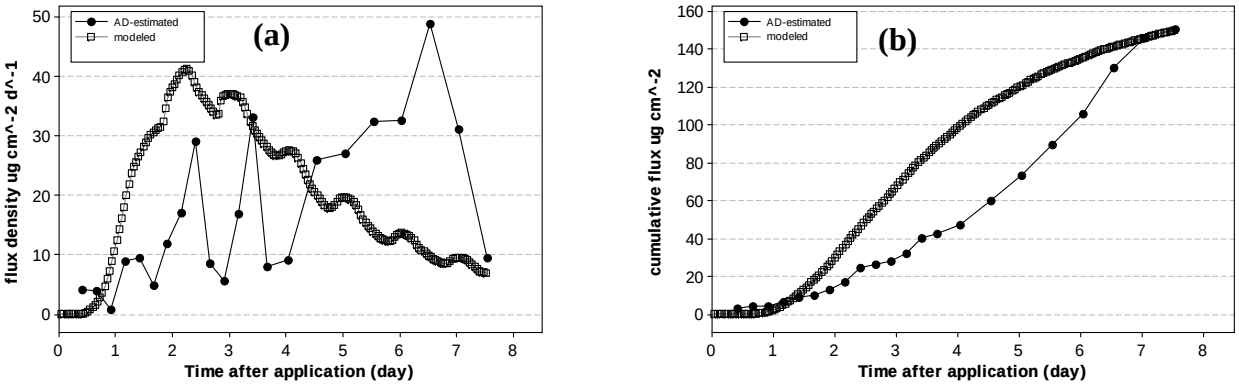

Figure 16. Modeled and AD-estimated (a) 1,3-D flux density, and (b) cumulative flux.

Two related factors also likely contributed to deviation between AD-estimated and modeled flux densities: (i) spatial variability in soil characteristics, and (ii) the very limited data available to characterize the soil. Four cores were taken for soil physical analysis in the 15 acre plot; these were composited into two cores before actual analysis for texture, 1/3 bar and 15 bar water contents (Table A-7, Appendix 1). The CVs for percent sand, silt and clay are relatively high at several depths, and a high level of variability in soil properties across the plot is also reflected in the variability in water contents across the field (Table 3). It is evident that two composite cores were inadequate to characterize the soil characteristics across the entire 15 acre field in the Imperial Study. One the other hand, even with extensive sampling and detailed soil characterization, it may not be possible to model fumigant volatilization at this site using a single deterministic simulation because soil conditions are highly variable.

Table 3. Coefficients of variation of measured soil properties in Imperial Study (N=2).

depth (cm)	Sand	Silt	Clay	1/3bar θ	15bar θ	OM	bulk density ρ_b
0-15	0.222	0.125	0.074	0.050	0.063	0.000	0.058
15-30	0.295	0.145	0.072	0.155	0.121	0.000	0.030
30-46	0.440	0.201	0.143	0.191	0.145	0.000	0.070
46-61	0.929	0.560	0.477	0.643	0.458	0.825	0.049
61-76	0.909	0.507	0.505	0.572	0.487	0.741	0.047
76-91	0.637	0.449	0.508	0.546	0.515	0.530	0.047

III. CONCLUSION

A. Study summary

- *Salinas* - HYDRUS-1D yielded predicted 1,3-D flux densities that agreed well with AD-estimated flux data.
    - Deviations between modeled and AD-estimated flux densities were likely within the range of error reported for the AD-estimation method.
    - The maximum AD-estimated flux occurred during the ninth sampling period. That 12-hr time-weighted average (TWA) estimated flux was 84.2 ug cm^{-2} d^{-1}. The corresponding maximum 12-hr TWA modeled flux was 65.6 ug cm^{-2} d^{-1}. The maximum 12-hr TWA modeled flux was calculated from 1-hr fluxes as the maximum of 12-hr running averages over the study duration.
    - The soil profile in the Salinas study was relatively coarse and homogeneous. These are optimum soil conditions for modeling gas phase diffusion.
- *Madera* - Actual 1,3-D volatilization was much more rapid than in the Salinas study or as predicted by HYDRUS2/3D.
    - Two potential causes of the observed rapid volatilization relative to model predictions were identified.
        - The empirical soil diffusion models that describe diffusion as a function of water content are only approximate because the effect of water content on pore connectivity and tortuosity varies from soil to soil. It may be that the Madera soil allows relatively rapid gas diffusion even at high water contents.
        - Some previous studies have theorized the presence of a “shank trace”, a high permeability channel penetrating the soil that is formed during fumigant application. Model simulations demonstrate that such a shank trace can produce rapid post-application volatilization behavior similar to that observed. However, no data were collected to support or refute this hypothesis, so the shank trace remains a hypothesis to be tested.
    - The maximum AD-estimated flux occurred approximately 48 hours after application. That 6-hr time-weighted average (TWA) estimated flux was

151 ug cm^{-2} d^{-1}. The corresponding maximum 6-hr TWA HYDRUS-modeled flux was 80 ug cm^{-2} d^{-1}.

- *Imperial* – 1,3-D volatilization was much slower than predicted by HYDRUS, and also much slower than typically observed in nearly all tarped and untarped 1,3-D fumigation studies in the literature.
    - There is no obvious single explanation for the slow volatilization. The high clay content and high water contents in the 15 – 30 cm and 30 – 45 cm subsurface layers likely contributed, but the 0 – 15 cm surface layer was much drier (Figure 14).
    - Error in the empirical soil diffusion (tortuosity) model may have contributed to differences between the modeled and AD-estimated flux data.
    - The field water content data and soil texture data indicated high spatial variability across the 15 acre field (Figure 14; Table 3). The number of soil samples taken to characterize the soil texture were inadequate. Error in parameterizing soil characteristics also likely contributed to differences between the modeled and AD-estimated flux data.
    - In addition, high variability in measured concentrations among replicate samples from different masts was also evident. These factors indicate that substantial flux estimation error $\varepsilon_{i,estimate}$ was likely.
    - The maximum AD-estimated flux occurred during the twenty second sampling period. That 12-hr time-weighted average (TWA) flux was 50 ug cm^{-2} d^{-1}. The corresponding maximum 12-hr TWA modeled flux was 40 ug cm^{-2} d^{-1}

B. Principal Findings

Based on the study by Majewski (1997), and the replicate air sampling conducted in the Imperial study, a lower bound estimate for mean AD-flux estimation error across sampling periods is on the order of 25% - 40%. Because neither estimate includes all sources of error, AD flux estimation error may be greater. It is important to understand flux estimation error because model performance is assessed relative to the estimated flux data. Failure to account for flux estimation error may lead to the erroneous assumption that deviations between modeled and estimated data are solely attributable to model inadequacy when, in fact, flux density estimation error may be comparable to or even dominate model error.

The HYDRUS models predicted the timing of peak flux in only one of the three studies. That study was conducted in Salinas on a coarse soil (sandy loam) that was relatively homogeneous These are the optimum soil conditions for modeling. Across all three studies, the maximum modeled flux densities averaged 71% of the AD-estimated fluxes (range 53 – 81%). Again however, our knowledge of AD estimation error is only poorly understood.

The “best-fit” soil degradation rates were remarkably similar in the three studies considering the diverse soil types. The corresponding half-lives were 5.8 days (Salinas), 5.6 days (Madera) and 5.1 days (Imperial).

From a model parameterization standpoint, sampling for soil physical characteristics (texture, water content as a function of matric potential, bulk density) was generally inadequate. This was a definite problem in the Imperial study given the spatial variability in water contents and soil properties (Table 3; Figure 14). In the Madera study, soil sampling for soil physical properties occurred at only one location where one sample was taken at each of 6 depths. Those samples were collected in a buffer zone that was *outside* the 9.93 acre test plot.

For fields with highly variable soil characteristics (such as in the Imperial Study), modeling approaches that rely on a single scenario comprised of an "average" soil may be inadequate. Alternate modeling approaches that rely on probabilistic approaches may be one alternative for those situations.

All mechanistic vadose zone transport models use empirical relationships to estimate soil diffusion coefficients from solute gas phase diffusion coefficients, water content and porosity. These relationships attempt to account for pore geometry effects, but provide only approximate estimates of the soil diffusion coefficient D_s. Error in D_s estimates may cause systematic deviations between HYDRUS modeled and field-based flux estimates. The available literature suggests the percent error in D_s estimates relative to actual D_s will be greatest in the wet soil range where D_s are smallest (e.g. Figure 11).

No relationship between barometric pressure fluctuations and 1,3-D volatilization was evident. In the Madera and Imperial studies, barometric pressure was actually increasing around the time of maximum flux density contrary to theoretical expectations. Thus, while barometric pressure may effect volatilization from soil under certain circumstances, there was no clear evidence of pressure-induced convective transport in the studies evaluated here.

bcc: Spurlock Surname File

REFERENCES

Atteia, O. and P. Hohener. 2010. Semianalytical model predicting transfer of volatile pollutants from groundwater to the soil surface. Environ. Sci. Technol. 44:6228-6232.

Auer, L.H., N.D. Rosenberg, K.H. Birdsell and E.M. Whitney. 1996. The effects of barometric pumping on contaminant transport. J. Contam. Hydrol. 24:145-166.

Chen, C.; Green, R. E.; Thomas, D. M.; Knuteson, J. A. 1995. Modeling 1,3-dichloropropene vapor-phase advection in the soil profile. Environ. Sci. Technol. 1995, 29, 1816–1821.

Chung S.-O., and R. Horton, Soil heat and water flow with a partial surface mulch, Water Resour. Res., 23(12), 2175-2186, 1987.

Creyer, S.A. and I .J. van Wesenbeeck. 2009. Estimating field volatility of soil fumigants using chain_2d: mitigation methods and comparison against chloropicrin and 1,3-dichloropropene field observations. Environ. Modeling Assess. 15:309-318

Footprint. Pesticide Properties Database. Available at: <http://sitem.herts.ac.uk/aeru/footprint/index2.htm>

Hilal, S.H., S.W. Karickhoff and L.A. Carreira. 2003a. Prediction of chemical reactivity parameters and physical properties of organic compounds from molecular structure using sparc. USEPA publication 600/R-03/030. Available at: <http://www.epa.gov/athens/publications/reports/EPA_600_R03_030.pdf>.

Hilal, S.H., S.W. Karickhoff and L.A. Carreira. 2003b. Verification and validation of the SPARC Model. USEPA publication 600/R-03/033. Available at: <http://www.epa.gov/athens/publications/reports/EPA_600_R03_033.pdf>.

Johnson, B. 2008. Dow Agrosciences-CHAIN2D Review. November 17, 2008 memorandum to J. Sanders. Available at: <http://www.cdpr.ca.gov/docs/emon/pubs/ehapreps/analysis_memos/2094_sanders.pdf>.

Kim, J-H, S.K. Paperniek, W.J. Farmer, J. Gan and S.R. Yates. 2003. Effect of formulation on the behavior of 1,3-dichloropropene in soil. J. Environ. Qual. 32:2223-2229.

Knuteson, J.A., D.G. Petty and B.A. Sherdut. 1992a. Field volatility of 1,3-dichloropropene in the Salinas Valley, California. DowElanco study ID ENV9011011.

Knuteson, J.A., D.G. Petty and B.A. Sherdut. 1992b. Field volatility of 1,3-dichloropropene in the Imperial Valley of Southern California. DowElanco study ID ENV91001.

Knuteson, J.A., Dixon-White, H.E. and D.G. Petty. 1995. Field volatility of 1,3-dichloropropene in San Joaquin Valley, California. Dowelanco study ID ENV93063.

Majewski,M.S. 1997. Error evaluation of methyl bromide aerodynamic flux measurements. In Fumigants: Environmental Fate, Exposure, and Analysis; Seiber, J. N., Knuteson, J. A., Woodrow, J. E., Wolfe, N. L.; Yates, M. V.; Yates, S. R., Eds.; ACS Symposium Series 652; American Chemical Society: Washington, DC; pp 135-153.

Massman, J. and D.F. Farrier. 1992. Effects of atmospheric pressure on gas transport in the vadose zone. Water Resour. Res. 28:777-791.

Meylan, W., P.H. Howard and R.S. Boethling. 1992. Molecular topology/fragment contribution method for predicting soil sorption coefficients, Environ. Sci. Technol. 26: 1560-7.

Moldrup, P., T. Olesen, J. Gamst, P. Schjonning, T. Yamaguchi, and D.E. Rolston. 2000. Predicting the gas diffusion coefficient in repacked soil: Water-induced linear reduction model. Soil Sci. Soc. Am. J. 64: 1588-1594.

Schaap, M.G., F.J Leij, M. Th. van Genuchten. 2001. ROSETTA: A computer program for estimating soil hydraulic parameters with hierarchical pedotransfer functions. J. Hydrol. 251:163-176.

Šimunek, J., M. Th. van Genuchten, and M. Šejna. 2005. The HYDRUS-1D software package for simulating the one-dimensional movement of water, heat, and multiple solutes in variably saturated media. Version 3.0, HYDRUS Software Series 1, Department of Environmental Sciences, University of California Riverside, Riverside, CA, 270 pp.

Šimunek, J., M. Th. van Genuchten, and M. Šejna. 2006. The HYDRUS software package for simulating two- and three-dimensional movement of water, heat, and multiple solutes in variably-saturated media, technical manual, Version 1.0, PC Progress, Prague, Czech Republic, 241 pp.

Spurlock, F. 2008. Fumigant transport modeling using HYDRUS: Estimation of soil hydraulic parameters using pedotransfer functions. August 14, 2008 memorandum to: R. Segawa. Available at: <http://www.cdpr.ca.gov/docs/emon/pubs/ehapreps/analysis_memos/2066_rosetta.pdf>

Spurlock, F. 2010. Fumigant transport modeling using HYDRUS: 3. Selection, temperature dependence and sensitivity analysis of fumigant physicochemical properties. Available at: <http://www.cdpr.ca.gov/docs/emon/pubs/ehapreps/analysis_memos/2077_segawa.pdf>

Thomas, J.E., L. H. Allen, L. A. McCormack, J. C. Vu, D.W. Dickson and L. Ou. 2003. Diffusion and emissions of 1,3-dichloropropene in Florida sandy soil in microplots affected by soil moisture, organic matter, and plastic film. Pest Manag Sci 60:390–398

Thorbjørn, A. P. Moldrup, H. Blendstrup, T. Komatsu and D. E. Rolston. 2008. A gas diffusivity model based on air-, solid-, and water-phase resistance in variably saturated soil. Vadose Zone J. 7:1276-1286.

van Dijk, H. 1980. Dissipation Rates in Soil of 1,2-Dichloropropane and 1,3- and 2,3-dichloropropenes. Pestic. Sci. 11:625–632.

van Genuchten, M. Th. 1980. A closed-form equation for predicting the hydraulic functions of unsaturated soils. Soil Sci. Soc. Am. J. 44:892-898.

van Genuchten, M. Th., F. J. Leij, and S. R. Yates. 1991. The RETC code for quantifying the hydraulic functions of unsaturated soils, Report No. EPA/600/2-91/065, R. S. Kerr Environmental Research Laboratory, U. S. Environmental Protection Agency, Ada, OK. 85 p.

van Wesenbeeck, I. J., J. A. Knuteson, D. E. Barnekow, and A. M. Phillips. 2007. Measuring Flux of Soil Fumigants Using the Aerodynamic and Dynamic Flux Chamber Methods. J. Environ. Qual. 36:613–620.

Wang, D., J.A. Knuteson, and S.R. Yates. 2000. Two-dimensional model simulation of 1,3-dichloropropene volatilization and transport in a field soil. J. Env. Qual. 29:639-644.

Wang, D., S.R. Yates and S. Gao. 2010. Chloropicrin emissions after shank injection: Two-dimensional analytical and numerical model simulations of different source methods and field measurements

Werner, D., P. Grathwohl, and P. Höhener, Review of field methods for the determination of the tortuosity and effective gas-phase diffusivity in the vadose zone, Vadose Zone J., 3,

1240-1248, 2004.

Wright, D.A., S.I. Sandler and D. DeVoll. 1992. Infinite dilution activity coefficients and solubilities of halogenated hydrocarbons in water at ambient temperatures. Environ. Sci. Technol. 26: 1828 – 1831.

Zheng, W., S. K. Papiernik, M. Guo, and S.R. Yates. 2003. Competitive degradation between the fumigants chloropicrin and 1,3-dichloropropene in unamended and amended soils. J. Env. Qual. 32:1735-1742.

SIMULATION OF THREE 1,3-DICHLOROPROPENE FLUX STUDIES USING HYDRUS

APPENDIX 1

1,3-D PHYSICAL-CHEMICAL PROPERTIES, SOIL-WATER PARAMETERS, SOIL SURFACE TEMPERATURE AND MODELING DOMAINS

I. Modeling Domains and General Boundary Conditions

Figure A-1. Salinas and Imperial Studies broadcast application - HYDRUS1D

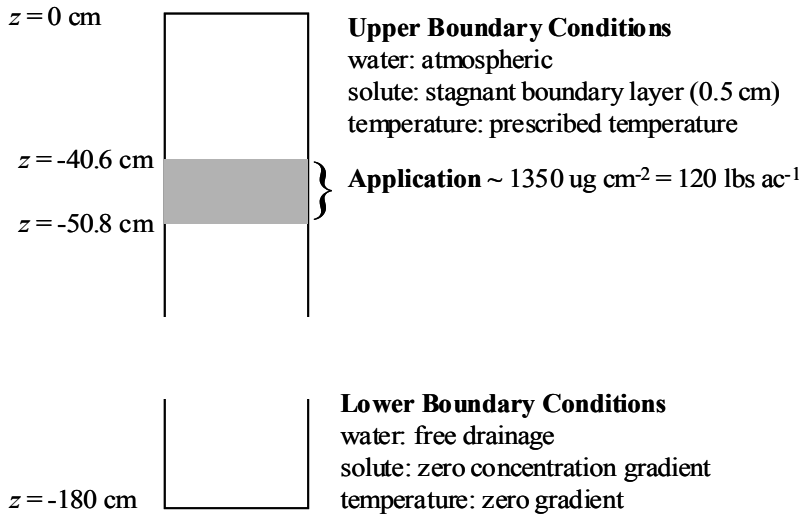

Figure A-2. Madera bedded row application - HYDRUS2/3D

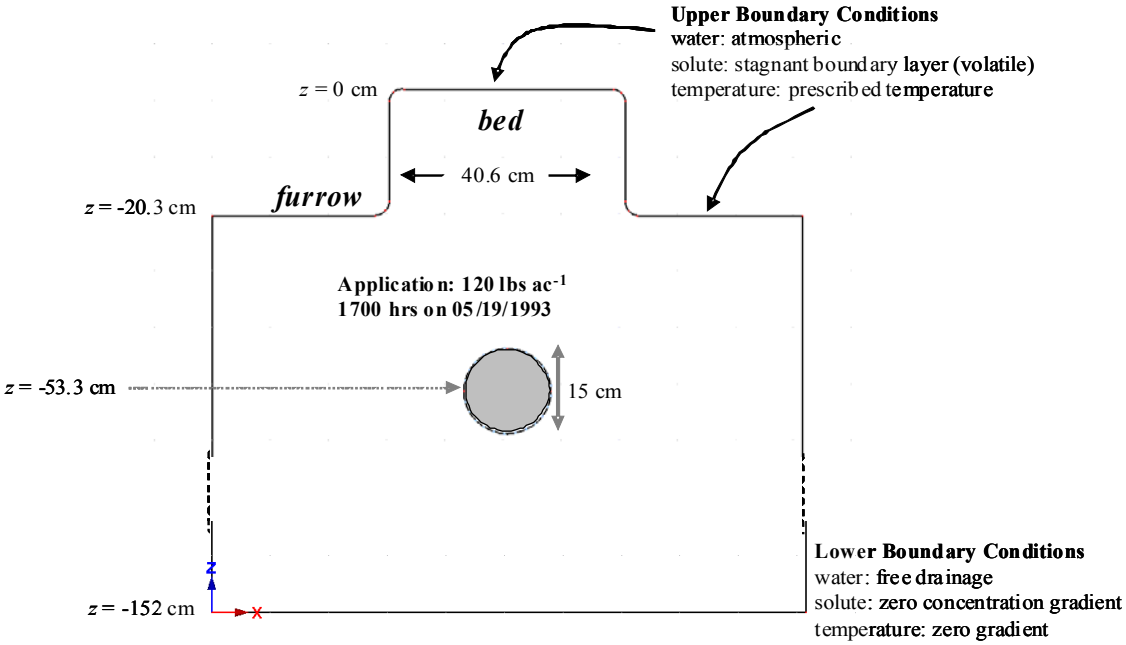

II. Soil Sampling for Physical Properties

A limited number of soil samples in each study were analyzed for texture, organic carbon and bulk density (ρ_b) (Table A-1, Table A-2). The soil analysis also included water

content at -0.3 bar ($\theta_{0.3\ bar}$) and -15 bar ($\theta_{15\ bar}$) matric potential in all 3 studies. Soil cores were collected for three purposes in each study: one or more cores for soil characterization (texture, organic carbon), a second set of core(s) for initial gravimetric water content, and a third core(s) for soil bulk density. In general, each type of core was collected in different part of the field plot. For example, in the Imperial study, bulk density cores were taken in the center of the experimental plot, while water content cores were taken from the center of each quadrant of the experimental plot. This is a source of uncertainty in volumetric water content calculations since that parameter is determined as the product of measured gravimetric water content and bulk density. Ideally both should be determined from measurements taken at the same location.

Table A-1. Number of cores/segments for initial water contents and soil physical characterization

Study	**# cores - length - segment length for soil physical characterization[A]**	**# cores - length - segment length for initial water content**
#1 - Salinas	4 - 90cm cores - 15cm segments	4 - 45cm cores - 15cm segments
#2 - Madera	1 - 90cm core -15cm segments	3 - 45cm cores - 15cm segments
#3 - Imperial	2 - 90cm cores - 15cm segments[B]	4 - 45cm cores - 15cm segments

[A] – texture, organic carbon and water retention data

[B] – each core was a composite of 2 cores

Table A-2. Number of cores - length - segment length for soil bulk density ρ_b

Study	**# cores/segments for soil bulk density ρ_b**
#1 - Salinas	4 - 60cm cores x 5cm segments
#2 - Madera	1 - 60cm core x 5cm segments
#3 - Imperial	4 - 60cm cores x 15cm segments

III. Soil Water Retention Functions

For the Salinas and Imperial studies, the van Genuchten (1980) soil-water retention curve parameters were estimated using the Rosetta pedotransfer function utility (PTF; Schaap et al., 2001) supplied with the HYDRUS model. The PTF inputs were % sand, % silt, % clay, ρ_b, $\theta_{0.3\ bar}$, and $\theta_{15\ bar}$. Among the PTF estimation methods available in Rosetta, this model yields the smallest error in estimated soil hydraulic parameters (Spurlock, 2008). In the Madera study, water content was also determined at matric potentials of -0.10 bar and –1.0 bar matric potential. These measured θ – matric potential data, along with a saturated volumetric water content estimated from measured ρ_b, were used to estimate

van Genuchten (1980) hydraulic parameters in the Madera study for each 15 cm soil layer using the nonlinear fitting program RETC (van Genuchten et al., 1991).

A. Soil data and van Genuchten (1980) parameters for the Salinas study.

Table A-3. Mean Salinas texture, organic carbon, bulk density (ρ_b, g cm^{-3}), 0.3 bar and 15 bar water content data by depth (standard deviation in parentheses, N=4). In the modeling simulations, all data for the 76.2 - 91.4 cm soil layer were assumed to represent soil characteristics down to the bottom of the modeling domain (152 cm).

	percent						
Depth (cm)	sand	silt	clay	org. C	ρ_b	0.3 bar θ	15 bar θ
0-15	66.9 (4.0)	19.3 (2.4)	13.9 (1.9)	0.50 (0.05)	1.46 (0.08)	12.6 (1.7)	5.4 (0.6)
15-30	72.1 (6.4)	16.5 (4.4)	11.4 (2.0)	0.36 (0.15)	1.50 (0.09)	11.4 (2.7)	4.7 (0.8)
30-46	81.9 (3.4)	10.8 (2.0)	7.4 (1.4)	0.23 (0.12)	1.55 (0.16)	8.5 (2.0)	3.4 (0.5)
46-61	73.4 (15.6)	18.5 (12.6)	8.2 (3.1)	0.30 (0.28)	1.45 (0.21)	11.2 (5.5)	4.2 (1.5)
61-76	73.1 (13.9)	19.8 (11.7)	7.2 (2.2)	0.25 (0.19)	1.49[A]	10.4 (3.6)	4.5 (1.3)
76-91	87.1 (5.3)	7.8 (3.4)	5.2 (2.5)	0.14 (0.06)	1.49[A]	6.8 (2.1)	3.6 (1.8)

[A] Soil bulk density ρ_b (g cm^{-3}) was only measured for 0 – 61 cm samples. The mean of all measured data (ρ_b =1.49) was assigned to layers below 61 cm.

Table A-4. Salinas soil hydraulic parameters estimated using Rosetta PTFs, and soil water distribution coefficient K_d (cm^3 g^{-1}, calculated assuming 1,3-D K_{OC} = 26).

Depth (cm)	θ_r	θ_s	α	n	K_s	K_d
0-15	0.0305	0.3875	0.0519	1.4431	131	0.13
15-30	0.0283	0.3796	0.0540	1.4640	153	0.09
30-46	0.0267	0.3685	0.0592	1.5904	256	0.06
46-61	0.0244	0.3867	0.0550	1.4511	152	0.08
61-76	0.0272	0.3737	0.0571	1.5214	140	0.06
76-180	0.0319	0.3853	0.0580	1.9569	492	0.04

Default heat capacities and thermal conductivity data for sandy soils based on Chung and Horton (1987) as provided in HYDRUS1-D were used for the Salinas study.

B. Soil data and van Genuchten parameters for the Madera study.

Table A-5. Madera texture, organic carbon, bulk density (ρ_b, g cm^{-3}), 0.1, 0.3, 1 and 15 bar volumetric water content data by depth. All data determined from one sample at each depth.

Depth (cm)	sand	silt	clay	org. C	ρ_b	0.1bar θ	0.3bar θ	1 bar θ	15 bar θ
0-15	51.2	31.6	17.2	0.73	1.12	0.300	0.232	0.139	0.075
15-30	49.2	31.6	19.2	0.70	1.58	0.385	0.346	0.195	0.123
30-46	51.2	31.6	17.2	0.38	1.54	0.370	0.330	0.209	0.120
46-61	47.2	37.6	16.2	0.32	1.53	0.408	0.320	0.182	0.114
61-76	43.2	35.8	21.2	0.25	1.58	0.386	0.346	0.209	0.123
76-91	47.2	33.6	19.2	0.32	1.31	0.398	0.353	0.197	0.117

Table A-6. Madera soil hydraulic parameters estimated from θ-matric potential data using RETC (van Genuchten et al., 1991). Soil water distribution coefficient K_d ($cm^3\ g^{-1}$) calculated assuming 1,3-D K_{OC} = 26.

Depth (cm)	θ_r	θ_s [A]	α	n	K_s	K_d
0-15	0.0211	0.5774	0.06951	1.34654	83	0.17
15-30	0.1202	0.4038	0.00253	2.34966	24	0.16
30-46	0.0000	0.4189	0.00740	1.28642	24	0.09
46-61	0.1110	0.4226	0.00347	2.16243	24	0.07
61-76	0.0000	0.4038	0.00448	1.31977	24	0.06
76-180	0.0604	0.5057	0.01035	1.43125	24	0.07

[A] - estimated from measured bulk density and assumed particle density ρ_p = 2.65 g cm^{-3} as $\theta_s = 1-\rho_b/\rho_p$

Default heat capacities and thermal conductivity data for loam soils based on Chung and Horton (1987) as provided in HYDRUS2/3D were used for the Madera study.

C. Soil data and van Genuchten parameters for the Imperial study**.**

Table A-7. Mean Imperial texture, organic carbon, bulk density (ρ_b, g cm^{-3}), 0.3 bar and 15 bar water content data by depth (standard deviation in parentheses, N=2). In the modeling simulations, all data for the 76.2 - 91.4 cm soil layer were assumed to represent soil characteristics down to the bottom of the modeling domain (152 cm).

	percent						
Depth (cm)	sand	silt	clay	org. C	ρ_b	0.3 bar θ	15 bar θ
0-15	31.8 (7.1)	39.5 (4.9)	28.7 (2.1)	0.54 (0.0)	1.33 (0.08)	25.7 (1.3)	11.3 (0.7)
15-30	28.8 (8.5)	45.7 (6.6)	25.5 (1.8)	0.24 (0.0)	1.44 (0.04)	27.9 (4.3)	11.7 (1.4)
30-46	29.6 (13.0)	50.6 (10.2)	19.8 (2.8)	0.15 (0.0)	1.37 (0.10)	22.2 (4.2)	8.8 (1.3)
46-61	36.7 (34.1)	47.0 (26.3)	16.3 (7.8)	0.07 (0.10)	1.29 (0.06)	18.7 (12.0)	6.6 (3.0)
61-76	35.8 (32.5)	47.4 (24.0)	16.8 (8.5)	0.06 (0.08)	1.36[A]	21.7 (12.4)	7.4 (3.6)
76-91	42.2 (26.9)	42.5 (19.1)	15.3 (7.8)	0.04 (0.04)	1.36[A]	18.3 (10.0)	6.4 (3.3)

[A] Soil bulk density ρ_b (g cm^{-3}) was only measured for 0 – 61 cm samples. The mean of all measured data (ρ_b =1.36) was assigned to layers below 61 cm.

Table A-8. Soil hydraulic parameters for Imperial study estimated using Rosetta PTFs, and soil water distribution coefficient K_d ($cm^3\ g^{-1}$, calculated assuming 1,3-D K_{OC} = 26).

Depth (cm)	θ_r	θ_s	α	n	K_s	K_d
0-15	0.0459	0.4243	0.0130	1.3891	21.5	0.14
15-30	0.0469	0.3994	0.0076	1.4438	12.3	0.06
30-46	0.0343	0.3916	0.0165	1.3842	22.5	0.04
46-61	0.0268	0.4015	0.0261	1.3698	32.3	0.02
61-76	0.0288	0.3878	0.0148	1.3986	26.7	0.01
76-180	0.0265	0.3875	0.0255	1.3708	33.4	0.01

Default heat capacities and thermal conductivity data for clay soils based on Chung and Horton (1987) as provided in HYDRUS1-D were used for the Imperial study.

Surface Temperature Boundary Condition

In the three DOW study reports, only a graphical presentation of soil temperature measured at the 2.5 cm depth was provided for each study. HYDRUS requires a specified soil surface boundary condition consisting of soil surface temperature as a function of time The procedure for estimating the actual soil surface temperature from the graphical 2.5 cm temperature data was as follows:

i. Convert the pdf plot of the 2.5 cm depth soil temperature time series to a bitmap.

ii. Increase the width of the sinusoidal temperature vs time curve on the bitmap by tracing using a drawing program.

iii. Import the modified bitmap into the digitizing program "Un-Scan It" (http://www.silkscientific.com/) and digitize. This procedure yields discrete (temperature, time) data pairs. For example, after digitizing, the 14.3 day Salinas data was comprised of 781 data, corresponding to a temperature for every ~ 26 minutes.

iv. Select the appropriate default soil thermal conductivity and heat capacity parameters (e.g. parameters for "sands", "loam" pr "clay" soils) in HYDRUS. Use the digitized measured temperature data from the 2.5cm depth as a time variable BC at the soil surface. When conducting this simulation, include an observation node at the 2.5 cm depth. This will provide 2.5 cm simulated temperature as output.

v. For the simulation in step iv., calculate the difference ΔT between the surface temperature used in that simulation (i.e. the actual measured temperature at the 2.5 cm depth) and the 2.5 cm depth simulated temperature at each of the 781 time points: $\Delta T = (T_{2.5cm,\ measured} - T_{2.5cm,\ simulation})$.

vi. Estimate actual surface temperature data as $T_{0cm} \cong T_{2.5cm,\ measured} + \Delta T$

vii. Re-run HYDRUS as in step iv using the estimate of T_{0cm} from step vi as the prescribed surface temperature BC. Compare the 2.5 cm depth temperature in this second simulation to $T_{2.5cm,\ measured}$ as a check of the overall procedure. Figure A-3 (a) and (b) compares $T_{2.5cm,\ measured}$ and $T_{2.5cm,\ simulation}$ for the Salinas data. The maximum absolute deviation between $T_{2.5cm,\ measured}$ and $T_{2.5cm,\ simulation2}$ in Figure A-3b was 1.00 degrees, while the median absolute difference was 0.05C.

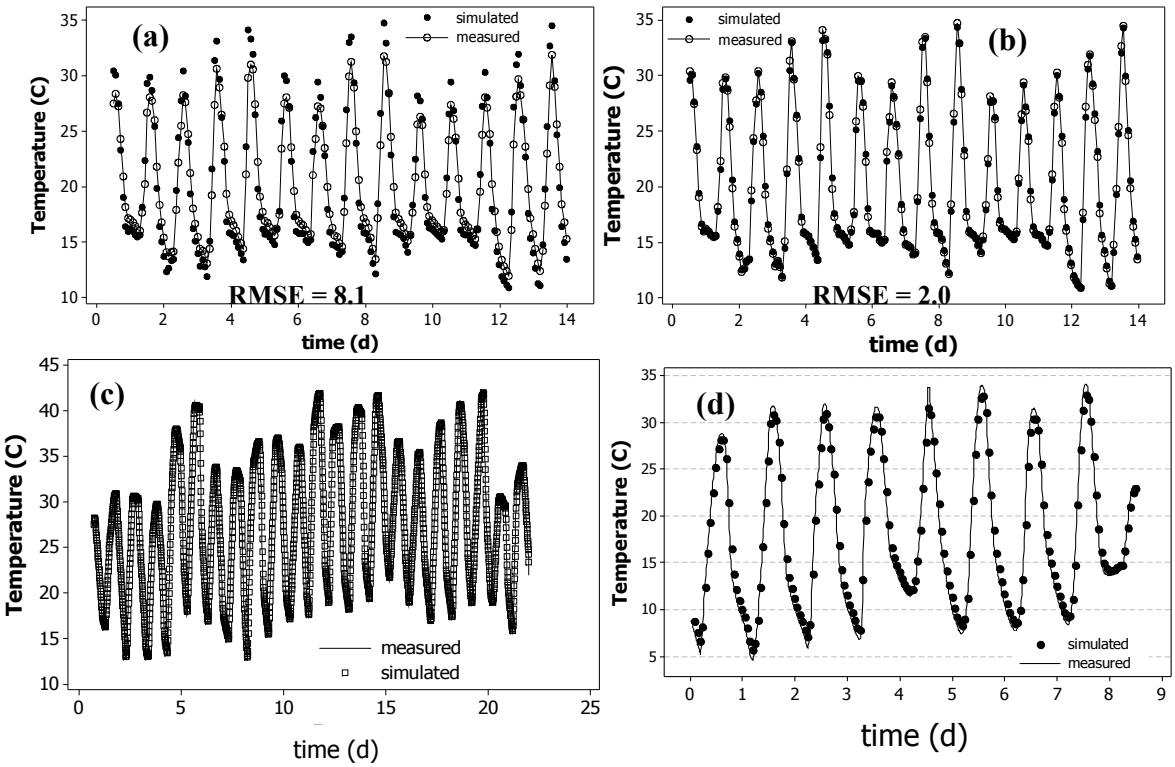

Figure A-3. (a) measured and simulated Salinas soil temperature at 2.5cm depth where the simulated assumed temperature at soil surface ≈ measured temperature at 2.5cm depth. **(b)** measured and simulated Salinas soil temperature at 2.5cm depth where the simulation used the estimated surface temperature BC (steps i - vii above). Note improved agreement between simulated and measured daily temperature maxima and minima. RMSE = root mean square error = $[1/N * \sum(T_{measured} - T_{simulated})^2]^{0.5} * 100/T_{mean}$; N = number of data = 781 for Salinas data set. **(c)** measured and simulated Madera soil temperature at 2.5cm depth using the estimated surface temperature BC. **(d)** measured and simulated Imperial soil temperature at 2.5cm depth using the estimated surface temperature BC.

<u>Evapotranspiration</u>

Preliminary simulations demonstrated that HYDRUS-simulated fluxes were relatively insensitive to daily evapotranspiration. Consequently the potential evaporation in each simulation was taken as the average evapotranspiration over the period of the study, as opposed entering the daily evapotranspiration as input. In each study, the mean evapotranspiration was in the range of ~ 0.3 - 0.4 cm day^{-1}. The historical data were acquired from weather stations Salinas.A (CIMIS #89), Madera.T and ElCentro.A (CIMIS #87), downloadable from http://www.ipm.ucdavis.edu/WEATHER/wxretrieve.html.

1,3-D Physical-Chemical Properties

Modeling procedures were essentially identical for all three datasets. With the exception of the first-order soil degradation rate constant, the 1,3-D physical-chemical properties were obtained from the literature (Table A-9). The activation energies are used by HYDRUS to calculate the temperature dependence of the Henry's constant and diffusion coefficients using an Arrhenius-type relationship (Šimunek et al., 2005).

Table A-9. 1,3-D Properties used in all modeling

Property	value	reference
aqueous phase diffusion coefficient D_w	0.735 $cm^2\ d^{-1}$	Hilal et al. 2003a, 2003b
gas phase diffusion coefficient D_0	6886 $cm^2\ d^{-1}$	Hilal et al. 2003a, 2003b
Henry's law constant K_H (20C)	0.055	FOOTPRINT, 2009
D_w activation energy	18035 J mol^{-1}	Hilal et al. 2003a, 2003b
D_0 activation energy	4560 J mol^{-1}	Hilal et al. 2003a, 2003b
K_H activation energy	32085 J mol^{-1}	Wright et al., 1992
K_{OC} sorption coefficient	26 L kg OC^{-1}	mean of 7 data from DPR PESTCHEM database

For all three datasets, vadose zone degradation of 1,3-D was modeled as a "lumped" process in the sense that the same degradation rate was assumed to apply to all phases in the soil: gas, solution and soil (sorbed). For the Salinas data, the lumped degradation rate constant was estimated using the nonlinear optimization program PEST (http://www.pesthomepage.org/Home.php). The "best-fit" k_1 was determined by minimizing sum of squared residuals between AD-estimated and HYDRUS-simulated cumulative 1,3-D flux. For the Madera and Imperial data, the optimum value of k_1 was chosen such that final AD-estimated and simulated cumulative fluxes were equal for the respective studies.